

THE 4TH INTERNATIONAL CONFERENCE ON ALUMINUM ALLOYS

EFFECTS OF THERMOMECHANICAL PROCESSING ON THE MICROSTRUCTURE OF Al-Li-Cu-Mg ALLOY (with < 1% Cr, Mn and Zr)

G. Avramovic-Cingara¹, H. J. McQueen², A. Hopkins³ and D. D. Perovic¹

1. Department of Metallurgy and Materials Science, University of Toronto, Toronto, Ont. M5S 1A4, Canada

2. Department of Mechanical Engineering, Concordia University, Montreal, Quebec H3G 1M8, Canada

3. University of Dayton Research Institute, Dayton, Ohio 45469-0130, USA

Abstract

As-cast and homogenized Al-Li-Cu-Mg-Mn-Cr (8090/Cr,Mn) alloy was subjected to torsional deformation at temperatures of 300, 400 and 500°C. Strain rates ranged between 0.01 and 5 s⁻¹. During these hot deformation processes, the dynamic recovery mechanism is active. The change in average subgrain size (d) with the condition of deformation (Z and σ_S) was quantitatively characterized. The deformation mechanism is strongly affected by the temperature of deformation. The difference in strain rates affects only the subgrain size. Alloys deformed at 300°C and 0.1s⁻¹ were aged at 185°C to the maximum hardness condition. The study was focused on examining subgrain substructure stability and the influence of particles on the dynamic recovery and/or static recrystallization mechanisms.

Introduction

Reducing the weight of aircraft structures through the exploitation of lighter advanced materials has always been a major target sought by the aircraft designer and producer. Among all technologies and candidate materials that promise weight savings, the new generation of Al-Li based alloys are particularly attractive to the aerospace industries because of their lower density and higher stiffness [1]. Therefore, over the last decade, increasing interest and extensive effort have been put into this research area to develop a new generation of Al-Li alloys [2,4-8]. The present research is designed to investigate the hotworkability and microstructural refinement in an Al-Li based alloy with minor additions of dispersoid-forming elements (Mn, Cr and Zr) based on both commercial interest and academic value. It is known that the function of such additions involves slip homogenization and ductility enhancement, as well as grain structure control, although depending on the nature of the particle/matrix interface, dispersoids may play an unfavorable role in the fracture process [2-4]. In this context, the study of hot deformation behaviour and quantitative characterization and understanding of microstructural changes accompanying dynamic and static restoration processes and precipitation is important.

EXPERIMENTAL

The current research study involves two different thermomechanical treatments: (i) isothermal continuous deformation [5,9,11] and (ii) ageing of previously deformed alloys.

The 8090/Cr,Mn alloy was provided by Kaiser Aluminium Co. The composition in weight percent was: 2.01Li-1.1Cu-0.88Mg-0.52Mn-0.14Cr-0.05Si-0.04Fe-0.03Ti-0.02Zr-0.015Zn. The torsion specimens with gauge length (L) of 25.4 mm and radius (r) of 3.16 mm were machined from an ingot homogenized at 538°C for 16 hrs and then cooled in air. The specimens were reheated to various deformation temperatures (T = 300, 400 and 500°C) in a radiant furnace in argon atmosphere, stabilized for 5 min. and deformed with different strain rates ($\dot{\epsilon} = 5, 1, 0.1$ and 0.01 s^{-1}) to fracture or true strain of 4. After deformation, the specimens were cooled in a water spray within 3 sec. Mechanical testing was performed on a computer directed, servocontrolled, hydraulic hot torsion machine. The von Mises equivalent flow stress, σ , and equivalent surface strain, ϵ , were derived by the standard equations:

$$\sigma = (\sqrt{3} M / 2\pi r^3) (3+n'+m) \quad (1)$$

$$\epsilon = 2\pi r / \sqrt{3} L \text{ (number of revolutions)} \quad (2)$$

where M is the torque, $m = \Delta \log M / \Delta \log \dot{\epsilon}$ is the strain rate sensitivity and $n' = \Delta \log M / \Delta \log \epsilon$ is the strain hardening coefficient [5]. Following hot working, the samples deformed at 300°C and 0.1 s^{-1} were aged in argon to the maximum hardness condition. They were subsequently solution treated at 545°C for 1 hr, quenched in water at 0°C and aged at 185°C for 44 hrs.

Transmission electron microscopy (TEM) was used to follow the microstructural changes and was performed on an HITACHI H-800 TEM/STEM instrument operating at 200 kV. Considering that the desired microstructure is produced only in the outer annulus of the torsional specimens, the samples for TEM were cut normal to the radius and just below the surface. The foils were mechanically ground on 600 grit SiC paper to 0.3 mm thickness, punched to 3 mm discs and subjected to double jet electro-polishing in Struers "Tenupol" in a solution of 1 part of HNO₃ and 3 parts of methanol cooled to about -30 °C at a voltage of 20 V. Subgrain sizes were determined using a planimetric method and were based on at least 3 samples or 10 micrographs. The subgrain misorientation angle was determined by observing the angle of rotation of the electron diffraction pattern on crossing a boundary. Only the trend in behaviour of grain boundary angles was analyzed. Standard imaging techniques were employed, i.e. bright field and superlattice dark field reflections.

RESULTS AND DISCUSSION

The stress-strain curves for 8090/Cr,Mn alloy are presented in Fig. 1. The curves are characterized by work hardening in the early stage of straining. Beyond a maximum (σ_p, ϵ_p), the flow stress decreases monotonically towards a steady state regime (σ_s), which is often not attained because of final fracture. The strain hardening rate, σ_p, ϵ_p and σ_s all decrease as T is raised and $\dot{\epsilon}(\text{s}^{-1})$ reduced. The peak behavior was observed in Al-Li based alloys for a wide range of deformation temperatures from 300 to 500°C and for all strain rates

investigated here. Nevertheless, the curves exhibit too great a decline beyond the peak, especially at 300°C, to be explained purely as a dynamic recovery (DRV) mechanism. However, the peaks are much broader than those due to classical dynamical recrystallization (DRX) observed in copper. The effect of temperature and strain rate on applied stress was analyzed by the following equation:

$$A (\sinh \alpha \sigma_p)^n = \dot{\epsilon} \exp (Q_{HW}/RT) = Z \quad (3)$$

where A , n , $\alpha = 0.052 \text{ MPa}^{-1}$, Q_{HW} and $R = 8.31 \text{ kJ/mol}$ are constants and Z is the Zener-Hollomon parameter. From the analysis given in reference [12], an activation energy of 185 kJ/molK was determined. The 8090/Cr,Mn alloy exhibits reasonable ductility at 300 and 400°C for all strain rates investigated here. At 500°C the ductility is somewhat reduced and reaches a maximum at $\dot{\epsilon} = 1 \text{ s}^{-1}$.

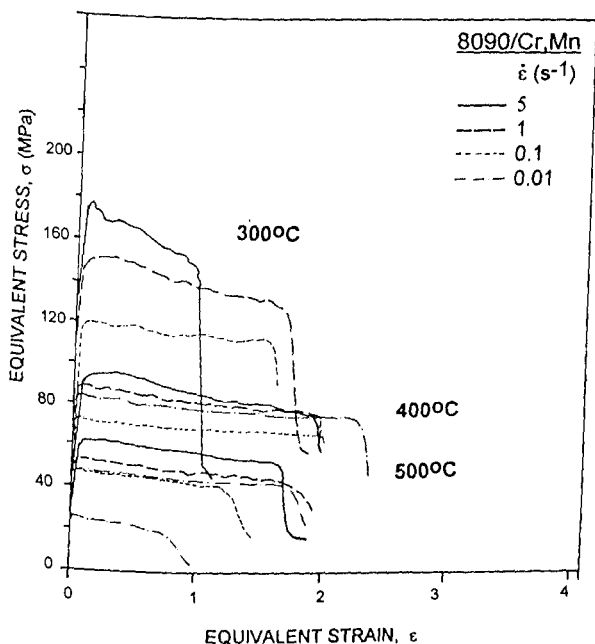


Figure 1. High temperature torsional equivalent stress vs. equivalent strain diagrams.

The microstructure of hot deformed 8090/Cr,Mn alloy over a wide range of temperatures and strain rates was examined. The substructure became more fully polygonized as the temperature increased and as the strain rate decreased, which is typical for aluminium alloys. However, the 8090/Cr,Mn alloy exhibited very well formed subgrains after deformation at 300°C for all strain rates investigated here. The microstructure of the alloy deformed at 300°C and 0.01 s⁻¹ is shown in Fig. 2(a). An example of the substructure after deformation with the highest strain rate of 5 s⁻¹ is given in the composite micrograph shown in Fig. 2(c). The subgrains are slightly elongated, but the substructure still exhibits an increasing level of dynamic recovery. This is consistent with mechanical behaviour during hot deformation. Dispersoids ranged in length from 0.2 to 0.5 μm and their average width was 0.1 μm. They were uniformly distributed, primarily at boundaries.

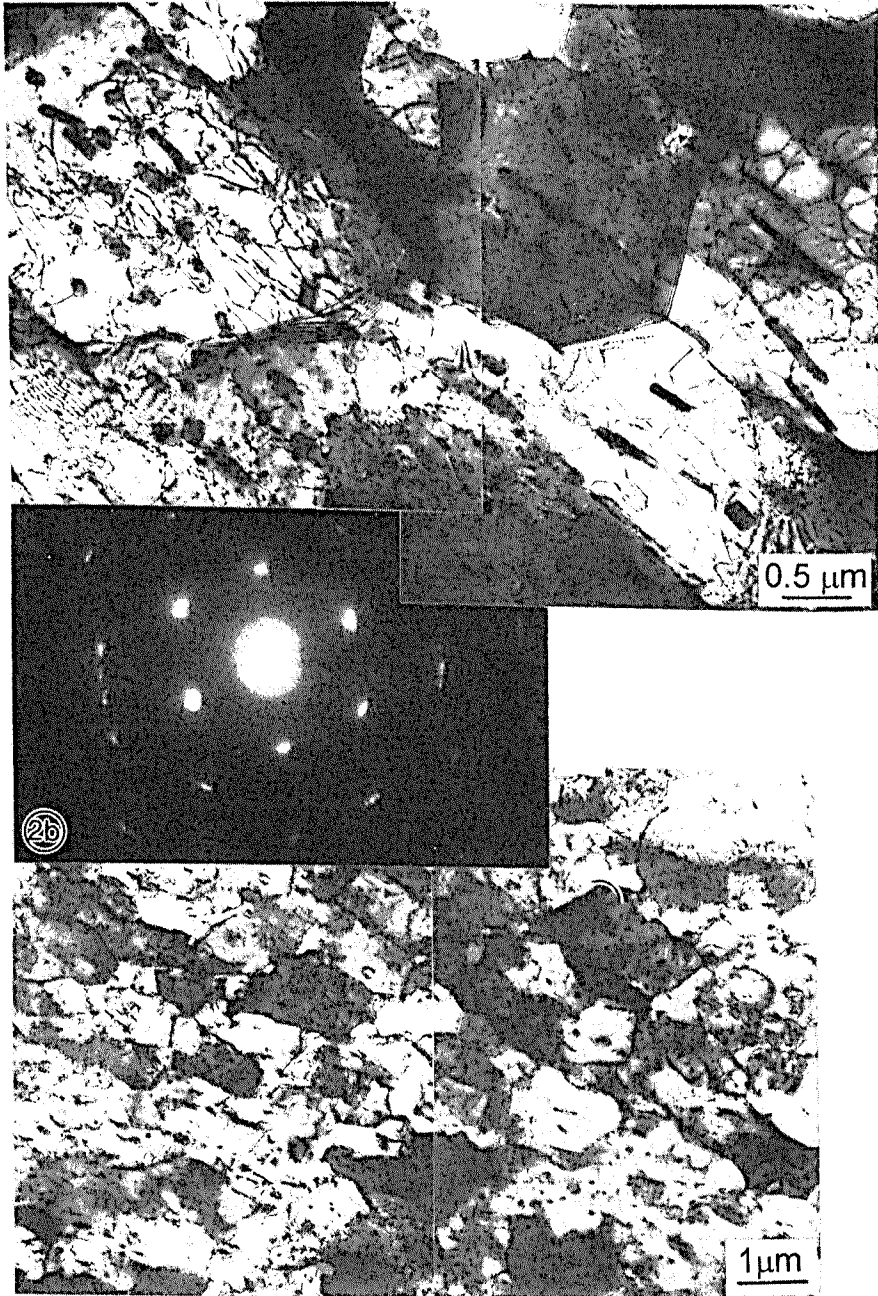


Figure 2. (a) Substructure of 8090/Cr,Mn alloy after deformation at 300°C and 0.01 s^{-1} ; (b) The SAD pattern indicates single crystal with subgrain misorientation angles of about 1.5 to 4 deg; (c) Very well formed subgrains after deformation at 300°C and 5 s^{-1} .

The average subgrain size was measured for a significant number of samples under different conditions. The subgrain average size ranges between 0.91 μm (for 300°C/5 s^{-1}) and 3.79 μm (for 400°C/0.01 s^{-1}), which is a characteristic of other aluminium alloys [7,10,11]. The subgrain diameter (d) varied uniformly with the condition of deformation, according to the relationship:

$$d^{-1} = 0.066 \ln Z - 1.663 \quad (4).$$

Fig. 3(a) shows the plot of $\ln Z$ vs. subgrain diameter. The data fit the regression lines quite well for all temperatures. The steady state flow stress is related to subgrain size by the following relationship (Fig. 3(b)):

$$\sigma_s = 142.95 d^{-1} - 5.276 \quad (5).$$

Subgrains are very well formed after deformation at 400°C, but it seems that the number of particles inside of subgrains is higher. After deformation at a strain rate of 0.01 s^{-1}

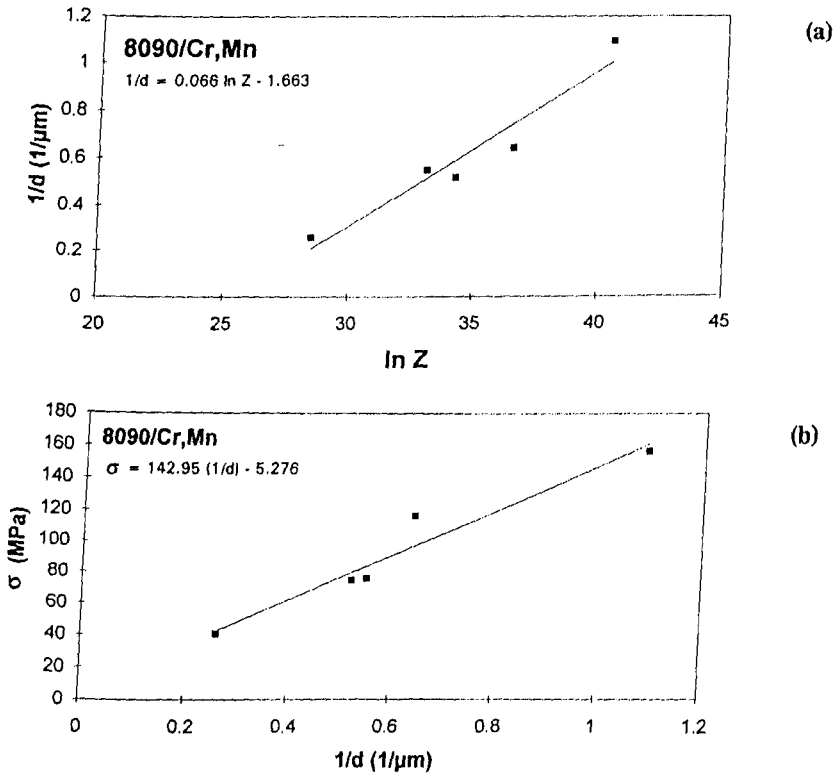


Figure 3. (a) Reciprocal subgrain diameter, d^{-1} ($1/\mu\text{m}$) vs. Zener-Hollomon parameter (Z);
 b) Reciprocal subgrain diameter, d^{-1} ($1/\mu\text{m}$) vs. steady state flow stress (σ_s).

the subgrains are almost equiaxed. The electron diffraction analysis indicated that this alloy contained low angle boundaries in all deformation conditions investigated here.

Micrographs of 8090/Cr,Mn alloy deformed at 300°C and 0.1 s^{-1} and aged at 185°C for 44 hrs are presented in Figs. 4 and 5. TEM analysis revealed a stable subgrain structure, that doubled in size (from 1.56 μm to 3.4 μm) with ageing. Fig. 4 illustrates subgrains within three grains, possessing the opposite contrast. This is an example of a serrated high angle grain boundary, which still exists after 44 hrs. of ageing treatment. The δ phase precipitates at high angle grain boundary, which is obvious from Fig. 4. These alloys exhibit precipitation of the T_1 -phase at low angle boundaries. The predominant strengthening precipitate is the δ' phase, which is uniformly dispersed throughout the matrix. The dark field image presented in Fig. 5(a) shows a copious δ' formation after deformation at 300°C and ageing. It seems that a bimodal distribution of δ' is developed here: small spherical precipitates and larger δ' particles that heterogeneously precipitated on Al_3Zr (β') [13]. The dark field image in Fig. 5(b) gives the evidence of precipitation of S-laths and T_1 -plates in a (110) matrix orientation (Fig. 5(c)). The S and T_1 phases can help to disperse intergranular planar slip thereby improving toughness without significantly reducing strength or ductility. Of the two phases present, a low volume fraction of S should be a more effective barrier to planar deformation than T_1 since the habit plane of S is not coincident with the matrix slip plane $\{111\}$ as is the case for the T_1 phase.

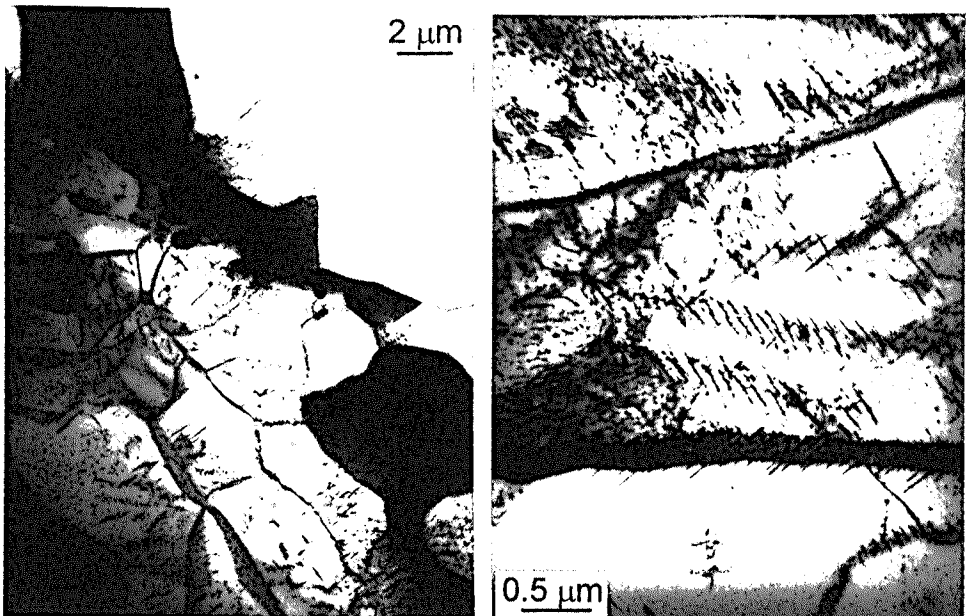


Figure 4. The 8090/Cr,Mn alloy deformed at 300°C (0.1 s^{-1}) and aged at 185°C (44 hrs). (a) The substructure inside of three grains. Serrated high angle grain boundary. The δ phase precipitates at high angle grain boundary; (b) Precipitation of T_1 phase on low angle boundaries.

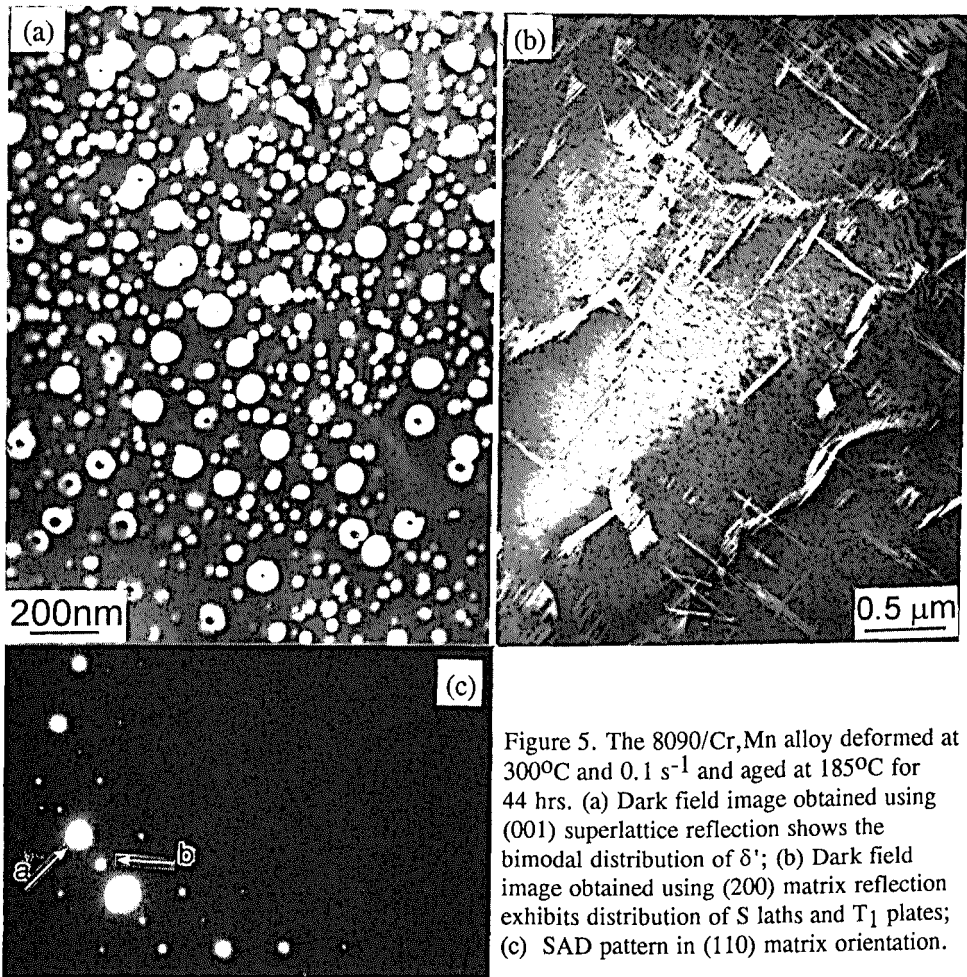


Figure 5. The 8090/Cr,Mn alloy deformed at 300°C and 0.1 s^{-1} and aged at 185°C for 44 hrs. (a) Dark field image obtained using (001) superlattice reflection shows the bimodal distribution of δ' ; (b) Dark field image obtained using (200) matrix reflection exhibits distribution of S laths and T_1 plates; (c) SAD pattern in (110) matrix orientation.

Dynamic recovery occurs to a high degree and leads to a steady state deformation in metals of high stacking fault energy, such as aluminium. The 8090/Cr,Mn alloy contains three classes of particles: coarse constituents (from casting), dispersoids and strengthening precipitates. Dispersoids normally precipitate during the homogenization treatment. These particles form from elements added to control grain size and/or suppress recrystallization (Cr, Mn, Zr) and thus serve as anchors for the subboundaries resulting in a stabilized substructure. In addition to dispersoids, there is some dynamic precipitation of second phase particles during deformation at high temperature. Deformation mechanisms are strongly affected by the temperature of deformation. Future work is necessary to explain the details of these mechanisms. In the case of isothermal continuous deformation of 8090/Cr,Mn alloy, dynamic recrystallization is entirely inhibited by dispersoids, second phase particles and solid solution effects. Finally, "static" precipitates formed during ageing nucleate at boundaries (δ) and subboundaries (T_1), thus stabilizing substructure as above and delay recrystallization.

CONCLUSIONS

An Al-Li-Cu-Mg-Cr-Mn-Zr alloy was subjected to continuous hot torsion deformation in the temperature range 300 - 500°C with strain rates in the range 0.01 to 5 s⁻¹. Systematic quantitative TEM study gives the evidence for the following conclusions:

- During continuous isothermal deformation, the mechanism of dynamic recovery is operative for all strain rates and deformation conditions investigated here. Subgrain sizes are related to deformation conditions according to the following relationships:
 $d^{-1} = 0.066 \ln Z - 1.663$; $\sigma_s = 142.95 d^{-1} - 5.276$.
The subgrain size is small and ranges between 1 and 5 μm. The 8090/Cr,Mn alloy exhibits very well formed and almost equiaxed subgrains after deformation at 300 and 400°C. Microstructural analysis is consistent with the mechanical behaviour.

After hot deformation at 300°C and 0.1 s⁻¹ worked alloys were aged at 185°C for 44 hrs. The major findings can be summarized as follows:

- Low angle boundaries and subgrains are still stable after long term ageing, even with an increased subgrain size. During ageing of these alloys, the mechanism of dynamic recovery is still active. After ageing the alloy exhibits a relatively uniform distribution of S, T₁, δ' and β' phases within subgrains. The δ phase precipitates at high angle grain boundaries, but there is evidence of a small amount of δ inside of the grains. The T₁ phase is present on low angle boundaries.

REFERENCES

1. R. H. Graham, R. J. Rioja and J. M. Newman, Aluminium Lithium Alloys VI, ed. M. Peters and P. J. Winkler, Garmisch-Partenkirchen, Germany, (1991), 15.
2. E. A. Starke, Jr., F. S. Lin, Metall. Trans., **13A**, (1982), 2259.
3. J. A. Walsh, K. V. Jata and E. A. Starke, Jr., Acta Metall. **37** (1989) 2861.
4. K. K. Sankaran, J. E. O'Neal and S. M. L. Sastry, Metall. Trans., **14A** (1983) 2174.
5. I. C. Smith, G. Avramovic-Cingara and H. J. McQueen, Aluminium- Lithium Alloys V, Williamsburg, Virginia, ed., T. H. Sanders and E. A. Starke, (1989), 223
6. G. Avramovic-Cingara and H. J. McQueen, Int. Conference on Advanced Aluminium and Magnesium Alloys, Amsterdam, (1993), ASM Int., 223.
7. G. Avramovic-Cingara and H. J. McQueen, The Strength of Metals and Alloys, (ICSM A 9), ed. D. G. Brandon, R. Chaim and A. Rosen, Haifa, (1991), 255.
8. H. J. McQueen, Hot deformation of Aluminium Alloys, ed., T. G. Langdon et al., TMS-AIME, Warrendale, PA, 1991, 31.
9. H. J. McQueen, K. Conrod and G. Avr.-Cingara, Can. Met. Quart., **32**, (1993), 375.
10. G. Avramovic-Cingara and H. J. McQueen, Pract. Metallography, **1**, (1993), 25
11. G. Avramovic-Cingara and H. J. McQueen, Aluminium, **70**, 3/4 (1994), 214.
12. H. J. McQueen, A. Hopkins, V. Jain, E. V. Konopleva and P. Sakaris, The 4th Int. Conf. on Aluminium Alloys (ICAA4), Atlanta, September, (1994) (to be published).
13. G. V. Gayle and J. B. Vander Sande, Scripta Metall., **18**, (1984), 473.
14. E. Nes and H. Bildal, Acta Metall., **25**, (1977), 1039.